Hasanov, Afig; Hasanov, Ruslan; Rustamov, Asad et al.

Article

Development of an axonometric model of photoelastic interaction in an acousto-optic delay line and its approbation

Technology audit and production reserves

Provided in Cooperation with:
ZBW OAS

Reference: Hasanov, Afig/Hasanov, Ruslan et. al. (2022). Development of an axonometric model of photoelastic interaction in an acousto-optic delay line and its approbation. In: Technology audit and production reserves 5 (2/67), S. 38 - 45. http://journals.uran.ua/tarp/article/download/267782/263814/618405. doi:10.15587/2706-5448.2022.267782.

This Version is available at:
http://hdl.handle.net/11159/12811

UDC 621.391.272
DOI: 10.15587/2706-5448.2022.267782
Article type «Reports on Research Projects»

Afig Hasanov,
Ruslan Hasanov,
Asad Rustamov,
Elgun Agayev,
Vugar Eynullayev,
Rovshan Ahmadov,
Masud Sadikhov

DEVELOPMENT OF AN AXONOMETRIC MODEL OF PHOTOELASTIC INTERACTION IN AN ACOUSTO-OPTIC DELAY LINE AND ITS APPROBATION

The object of research is a mathematical model of the photoelastic interaction in an acousto-optic delay line (AODL). Two possible cases are discussed as applied to the ratio of the input pulse duration to the time of crossing the optical beam by an elastic wave packet. It is shown that in both cases the voltage at the output of the device is found as the sum of three components, which are formed by different mechanisms. If the duration of the input pulse is longer than the time of crossing the optical beam by an elastic wave packet, then the first component is determined by the process of entry of the leading edge of the elastic wave packet into the optical beam, the second – by the process of complete interaction of the optical beam with the elastic wave packet, and the third – by the process of exit of the trailing edge of the elastic wave packet from the optical beam. In the second case, i. e. when the duration of the input pulse is less than the time of crossing the optical beam by an elastic wave packet, the first term is determined by the process of entry of the elastic wave packet into the optical beam, the second – by the process of advancing the elastic wave packet in the aperture of the optical beam, and the third – by the process of exit of the elastic wave packet from the aperture of the optical beam. The corresponding equations for calculating the parameters of the output pulse were obtained by applying a rectangular pulse to the AODL input. It is proved that if the pulse duration at the AODL input is longer than the time of intersection of the optical beam by an elastic wave packet, then the pulse duration at its output will be equal to the duration of the input pulse. In the case when the duration of the input pulse is less than the time of crossing the optical beam by an elastic wave packet, the duration of the output pulse will be determined by the time of propagation of the elastic wave packet in the aperture of the optical beam. The obtained equations are confirmed by numerical calculations. The results of the numerical analysis were tested experimentally, which confirms the unequivocal adequacy of the proposed model of photoelastic interaction in an AODL.

Keywords: *delay line, axonometric projection, optical beam, elastic wave, pulse duration, time domain, Bragg angle.*

Received date: 09.11.2022
Accepted date: 24.11.2022
Published date: 25.11.2022

How to cite
Hasanov, A., Hasanov, R., Rustamov, A., Agayev, E., Eynullayev, V., Ahmadov, R., Sadikhov, M. (2022). Development of an axonometric model of photoelastic interaction in an acousto-optic delay line and its approbation. Technology Audit and Production Reserves, 5 (2 (67)), 38–45. doi: https://doi.org/10.15587/2706-5448.2022.267782

1. Introduction

Signal processing in the time domain is one of the necessary operations in many radio-engineering systems. To solve this problem, electromagnetic, acoustic, digital and optical delay lines (DL) are more often used [1–4]. In [1], a continuously tuned dispersive DL is presented. Here, the base unit consists of a stepped resistance section and two variable resistors in the form of *p-i-n* diodes. The use of this DL provides fast tuning in a given frequency range. In [2], a low-loss acoustic DL based on transverse horizontal waves in a thin film of lithium niobate ($LiNbO_3$) is demonstrated. In [3], a digital DL with multiple inputs is described to ensure operation in a wide frequency range. In [4], a tunable optical DL is discussed, which allows one to choose time delays of 110, 225, and 330 ps.

In all types of DL, the signal delay is due to the finite speed of the physical processes occurring in them. The fact that the speed of propagation of acoustic oscillations is about 10^5 times less than that of electromagnetic ones explains the undeniable advantages of acoustic DL in comparison with electromagnetic and optical ones when it is necessary to obtain large delays in analog signals. The impossibility of obtaining a smoothly controlled signal delay is a significant drawback of acoustic DL. Smoothly controlled signal delay up to several hundreds of nanoseconds is achieved using an electromagnetic DL.

Adjustable delay can be obtained using digital DL. In these devices, the analog signal is sampled, quantized and, after encoding, converted into a digital signal, which is

entered into a memory device (memory), and then output from the memory and converted into an analog signal. The disadvantages of digital DL are: the presence of quantization errors, aperture errors, etc.; the difficulty of creating analog-to-digital and digital-to-analog converters with high speed; narrowband, etc.

Signal processing in the time domain is used, for example, in the implementation of matched filters, radar simulators [5, 6], and signal generators of various shapes are built on their basis [7, 8]. In [5], a linear invariant filter is presented, in which the required time interval is formed by an electromagnetic DL implemented on the basis of *LC* and *RC* chains. In [6], the implementation of a radar simulator based on a digital DL is discussed. In [7], a high-frequency generator based on a broadband acoustic DL made of $LiNbO_3$ is described. In [8], a compact triangular-shaped signal generator with broadband tuning is described, the main element of which is an optical DL.

From the analysis of the manufacturing technology, as well as specific applications of the above-mentioned DL, it is obvious that they cannot be used for a smoothly controlled delay of broadband analog signals over a wide range, for example, up to several tens of microseconds. In the context of solving such a problem, the photoelastic effect has a high potential [9–12]. In [9], the possibility of using the features of the photoelastic effect to construct broadband delay lines is discussed. The potential possibilities of an acousto-optic delay line are discussed in [10] in the context of the formation of a sequence of ultrashort laser pulses. In [11], the features of the photoelastic effect are used to delay femtosecond pulses up to 6 picoseconds with high accuracy. In [12], the results of picosecond optoacoustic experiments are presented.

A device that is implemented on the basis of the photoelastic effect and provides signal processing in the time domain is commonly called an acousto-optic delay line (AODL). In devices of this class, efficient signal processing in the time domain is due to the low propagation velocity of an acoustic wave in a photoelastic medium (PEM) and the possibility of synthesizing PEM of sufficiently large sizes. At the same time, the low propagation velocity of an elastic wave predetermines the geometric and energy parameters of the photoelastic interaction, since it crosses the optical beam at the same speed [13].

The photoelastic effect is realized in an acousto-optic modulator (AOM), which consists of PEM and an electroacoustic transducer (EAT) attached to its end (Fig. 1). The thickness of the EAT depends on the operating frequency and can range from a few microns to a few millimeters. It should be noted that AOM-based acousto-optic processors have a high potential in the context of processing broadband analog signals. The AOM operating frequency range is 40–60 percent of its central frequency, which is selected in the range from tens of MHz to units of GHz.

The signal processed in AODL in most cases is pulsed [14]. At the same time, the diameter of the optical beam has finite dimensions. Therefore, the design, development, and adjustment of AODL in all cases requires matching the duration of the input pulse signal τ_i with the velocity of propagation of an elastic wave in the PEM υ and the diameter of the light beam d.

The known theories of photoelastic interaction are quite complex in the context of adaptation to the development of AODL with specified parameters [15, 16]. All this determines the relevance of developing such a theoretical model of photoelastic interaction in AODL, which is available for applied applications. In the context of solving the formulated problem, it is taken as a basis that the use of axonometric projection makes it possible to increase the visibility of photoelastic interaction.

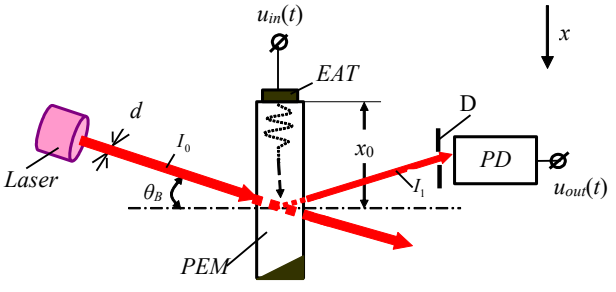

Fig. 1. Structural diagram of AODL

Thus, *the object of research* is a mathematical model of the photoelastic interaction in an acousto-optic delay line (AODL).

The aim of this research is to create a mathematical model of the photoelastic interaction based on its axonometric projection and to derive calculated ratios to assess the limiting capabilities of AODL.

2. Materials and Methods

The studies were carried out by theoretical and numerical methods, the results of which were tested experimentally.

An electric signal $u_{in}(t)$ with a carrier frequency f_0 in the range from tens of MHz to a few GHz is supplied to the EAT terminals, which excites an elastic wave in the PEM with a power P_a and with cross-sectional dimensions equal to the length L and width H of the EAT, respectively. When the laser beam falls into the PEM aperture (in this case at the Bragg angle, θ_B), a photoelastic effect is observed, i. e. part of the light is deflected. In the case of Bragg diffraction, only one diffraction order is observed. The spatial position of the deflected beam and the light intensity in it is determined by the parameters of the radio frequency electrical signal connected to the terminals of the EAT [17]. The deflected light beam passes through a slit in the diaphragm (D) and is recorded by a photodetector (PD). The signal at the PD output $u_{out}(t)$ lags behind the input signal $u_{in}(t)$ by time $\tau=x_0/\upsilon$, where x_0 is the distance from the EAT to the acousto-optic interaction point. The desired signal delay $u_{in}(t)$ is set by changing x_0. It is on this principle that AODL is implemented, in which the photoelastic interaction occurs within the limits of the laser beam aperture.

Fig. 1 illustrates the Bragg diffraction mode, in which laser radiation with power P_0, wavelength λ and frequency v falls into the PEM aperture at the Bragg angle $\theta_B=\arcsin(0.5\lambda/\Lambda)$, where $\Lambda=\upsilon/f_0$ is the elastic wave length.

As a rule, a weak acousto-optic interaction is used in AODL. Therefore, it is possible to assume that the intensities of the incident light I_0 and the deflected light I_1 are related by the following approximate equality [18]:

$$I_1 \approx I_0 \cdot \eta, \quad (1)$$

where $\eta=[\pi^2 M P_a L]/(2\lambda^2 H)$ – the diffraction efficiency; $M=n^6 p^2/(\rho\upsilon^3)$ – quality factor of PEM; n, ρ and p are the

ISSN 2664-9969

refractive index, density and photo-elastic constant of the interaction medium, respectively.

To simplify the interpretation of the mechanism of formation of the output voltage $u_{out}(t)$, let's assume that the power flux density is uniformly distributed in the laser beam cross section. Let's also assume that a photomultiplier tube (PMT) is used as a PD.

Taking into account the accepted initial conditions, the power of the deflected light beam P_1 is determined on the basis of formula (1) in the stationary mode, i. e. when the light beam fully interacts with an unmodulated elastic wave packet and the cross-sectional area of the deflected light beam S_1 remains unchanged:

$$P_1 = S_1 I_1 = S_1 I_0 \eta = S_1 \eta P_0 / S_0, \quad (2)$$

where S_0 – the cross-sectional area of the light beam incident into the AOM aperture.

Let's note that in any case, the cross-sectional area of the deflected light beam is equal to the cross-sectional area of the acousto-optic interaction in the collinear plane.

The deflected light beam through the aperture in the diaphragm falls on the photosensitive surface of the PMT. The current at the output of the PMT is determined according to the laws of general physics as follows:

$$i_{out} = Ge\eta' P_1/(h\nu), \quad (3)$$

where G – PMT gain; $e = 1.6 \cdot 10^{-19}$ C – proton charge; η' – quantum yield of the photocathode (the average number of electrons emitted by the photocathode when one photon falls on it); $h = 6.63 \cdot 10^{-34}$ $J \cdot s$ – Planck's constant. Let's note that in this case, the number of photons incident per second on the photosensitive PMT surface is equal to $P_1/(h\nu)$.

Based on expressions (1)–(3), let's write the formula for the voltage at the PMT load with resistance R_L:

$$u_{out} = R_L \cdot i_{out} = R_L Ge\eta' S_1 \eta P_0/(S_0 h\nu). \quad (4)$$

In photoelastic interaction, the stationary regime with all its attributes is established only under certain conditions. On the whole, the cross-sectional area of the acousto-optic interaction, respectively, the cross-sectional area of the deflected light beam S_1, and the PMT output voltage u_{out} are functions of the current x coordinate. Therefore, let'sd rewrite formula (4) as a function of the x coordinates in the following form:

$$u_{out}(x) = cS_1(x), \quad (5)$$

where $c = R_L Ge\eta' \eta P_0/(S_0 h\nu)$ is a constant multiplier for the selected AODL design, with the dimension V/m^2.

In accordance with the above statement, when modeling the process of photoelastic interaction in AODL, it is possible to assume that a pulse signal of duration τ_i arrives at its input. In this case, two cases are possible:

a) the duration of the input pulse signal is longer than the time of crossing the laser beam by the acoustic wave packet, $\tau_i > d/\upsilon$;

b) the duration of the input pulse signal is less than the time of crossing the laser beam by the acoustic wave packet, $\tau_i < d/\upsilon$.

For the selected design of AODL, the parameters d and υ remain unchanged. Therefore, to assess the limiting capabilities of a particular sample of AODL, it is convenient to introduce the parameter $\tau_0 = d/\upsilon$, which is equal to the time of establishment of a stationary mode, at $\tau_i > d/\upsilon$.

In both cases, the duration of the acousto-optic interaction is equal to $\tau_i + \tau_0$. However, the pulse duration at the PMT output will be determined in the first case as $\tau_{out} = \tau_i$, and in the second case as $\tau_{out} = \tau_0$. In addition, the mechanism of pulse formation at the PMT output in the first and second cases differs significantly.

The axonometric projection of the photoelastic interaction for the case when the duration of the input pulse is longer than the time of crossing the laser beam by the acoustic wave packet, i. e. when $\tau_i > \tau_0$ is shown in Fig. 2. Under these conditions, the leading and trailing fronts of the pulse at the PMT output are formed by the process of entry and exit of the leading and trailing fronts of the elastic wave packet into the optical beam, respectively.

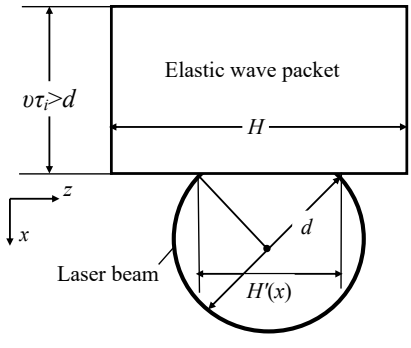

Fig. 2. Axonometric projection of the photoelastic interaction on a plane perpendicular to the direction of propagation of the laser beam, for the case when the pulse duration $\tau_i > \tau_0$

When the leading edge of the elastic wave packet enters the optical beam, the process of changing the cross-sectional area of the deflected light beam is modeled by the following equation:

$$S_{11}(x) = \int_{x_0}^{x} H'(x)\mathrm{d}x, \text{ by } x_0 \le x \le x_0 + d, \quad (6)$$

where the length of the interaction line of the leading edge of an elastic wave packet with a laser beam in the xoz plane:

$$H'(x) = 2[d(x - x_0) - (x - x_0)^2]^{0.5}, \text{ by } x_0 \le x \le x_0 + d. \quad (7)$$

At $x = x_0 + d$, the area of acousto-optic interaction will have a maximum value and is defined as:

$$S_{12}(x)\big|_{x=x_0+d} = \int_{x_0}^{x_0+d} H'(x)\mathrm{d}x = 0.25\pi d^2, \text{ by } x_0 + d \le x \le x_0 + \upsilon\tau_i. \quad (8)$$

The value of the cross-sectional area of the deflected light beam, determined by formula (8), will remain until the leading edge of the elastic wave packet reaches the distance $x = x_0 + \upsilon\tau_i$. Then the process of exit of the elastic wave packet from the optical beam begins, which is accompanied by a decrease in the cross-sectional area of the deflected light beam. Under these conditions, the cross-sectional area of the deflected light beam is given by:

$$S_{13}(x)=\int_{x_0}^{x_0+d} H'(x)\mathrm{d}x-\int_{x_0}^{x-\upsilon\tau_i} H'(x)\mathrm{d}x,$$

by $x_0+\upsilon\tau_i\le x\le x_0+\upsilon\tau_i+d$. (9)

The above interpretation of the photoelastic interaction allows to conclude that the change in the cross-sectional area of the deflected light beam occurs in accordance with equations (6), (8) and (9). Therefore, when the AODL input is exposed to a signal in the form of a rectangular pulse (in this case, with a duration $\tau_i>\tau_0$), the voltage at its output will be determined by the sum of three terms.

Taking into account the fact that in the case under consideration the current coordinate x is related to the current time t by the equality $x=\upsilon\cdot t$, equations (6)–(9) can be transferred to the time plane in the following form:

$$H'(t)=2\upsilon[(d/\upsilon)(t-\tau)-(t-\tau)^2]^{0.5},\ \text{by}\ \tau\le t\le\tau+\tau_0. \quad (10)$$

$$S_{11}(t)=\upsilon\cdot\int_{\tau}^{t} H'(t)\mathrm{d}t,\ \text{by}\ \tau\le t\le\tau+\tau 0. \quad (11)$$

$$S_{12}(t)\big|_{t=\tau+d/\upsilon}=\upsilon\int_{\tau}^{\tau+d/\upsilon} H'(t)\mathrm{d}t=0.25\pi d^2,$$

by $\tau+\tau_0\le t\le\tau+\tau_i$. (12)

$$S_{13}(t)=\upsilon\int_{\tau}^{\tau+d/\upsilon} H'(t)\mathrm{d}t-\upsilon\int_{\tau}^{t-\tau_i} H'(t)\mathrm{d}t,$$

by $\tau+\tau_i\le t\le\tau+\tau_i+\tau_0$. (13)

In accordance with the above, the voltage at the PMT output will be formed as the sum of three components. Based on equations (5), (10)–(13), let's obtain the following equations for the voltage components at the PMT output:

$$u_{out.1}(t)=c\upsilon\int_{\tau}^{t} H'(t)\mathrm{d}t,\ \text{by}\ \tau\le t\le\tau+\tau_0. \quad (14)$$

$$u_{out.2}(t)=c\upsilon\int_{\tau}^{\tau+d/\upsilon} H'(t)\mathrm{d}t,\ \text{by}\ \tau+\tau_0\le t\le\tau+\tau_i. \quad (15)$$

$$u_{out.3}(t)=c\upsilon\left[\int_{\tau}^{\tau+d/\upsilon} H'(t)\mathrm{d}t-\int_{\tau}^{t-\tau_i} H'(t)\mathrm{d}t\right],$$

by $\tau+\tau_i\le t\le\tau+\tau_i+\tau_0$. (16)

The resulting equation for the voltage at the output of the PMT will have the following form:

$$u_{out}(t)=u_{out.1}(t)+u_{out.2}(t)+u_{out.3}(t),\ \text{by}\ \tau\le t\le\tau+\tau_i+\tau_0. \quad (17)$$

From the joint analysis of equations (14)–(17), let's obtain the following formula for calculating the voltage at the PMT output:

$$u_{out}(t)=u_{out.1}(t)\cdot[\Phi(t-\tau)-\Phi(t-\tau-\tau_0)]+$$
$$+u_{out.2}(t)\cdot[\Phi(t-\tau-\tau_0)-\Phi(t-\tau-\tau_i)]+$$
$$+u_{out.3}(t)\cdot[\Phi(t-\tau-\tau_i)-\Phi(t-\tau-\tau_i-\tau_0)],$$
by $\tau\le t\le\tau+\tau_i+\tau_0$, (18)

where $\Phi(t)$ – Heaviside unit function.

Summarizing the accepted conditions, the established regularities and the results obtained, it can be postulated that when the inequality $\tau_i>\tau_0$ is satisfied, the shape and parameters of the response of the AODL to a rectangular input action can be calculated using formula (18).

Numerical simulation of the AODL reaction with parameters: d=1.6 mm; υ=3.63 km/s; τ=0.5 μs to a rectangular input effect with a duration of τ_i=1.5 μs. The calculation is carried out according to the formula (18). The calculation results are presented in Fig. 3, in the form of a normalized graph of the voltage at the output of the PMT.

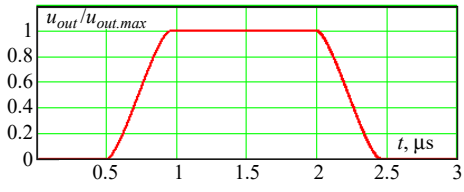

Fig. 3. Normalized graph of the voltage at the output of AODL with the duration of the input pulse τ_i=1.5 μs

According to the graph in Fig. 3, the rise (fall) time is determined, which is equal to 0.44 μs and coincides with the calculated value τ_0=0.444 μs. The pulse duration is 1.5 μs (defined at level 0.5), which also corresponds to the above position.

The above approach to analyzing the features of the photoelastic interaction was used in [19] to study the temporal and frequency characteristics of AODL. Here, the cutoff frequency of the AODL with direct detection is determined from the rise time of the pulse at the output. In the same place, the result obtained was confirmed by numerical simulation and tested experimentally.

Let's now consider the case when the duration of the input pulse is less than the time of crossing the laser beam by the acoustic wave packet, i. e. when $\tau_i<\tau_0$. Some aspects of this operating mode of the AODL are discussed in [20].

Fig. 4 shows an axonometric projection of the interaction of an elastic wave packet with a duration $\tau_i<\tau_0$ and a width H with an optical beam with a diameter d onto the xoz plane.

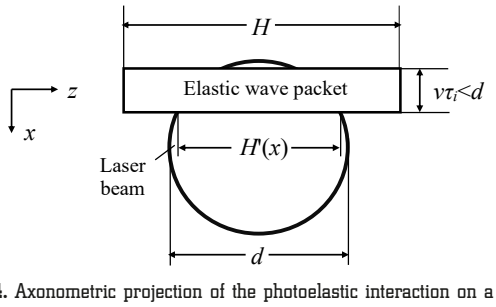

Fig. 4. Axonometric projection of the photoelastic interaction on a plane perpendicular to the direction of laser beam propagation for the case when the pulse duration $\tau_i<\tau_0$

Under these conditions, if to assume that the coordinate system moves along the x axis with a speed υ, then the AODL can be considered as a linear stationary system with a rectangular impulse response of duration τ_i. Such an interpretation of physical processes allows accepting that the optical beam enters the above linear stationary system with a velocity υ. In this case, the acousto-optic interaction includes only that part of the optical beam that is within the cross-sectional area equal to:

ISSN 2664-9969

$$S_1(x)=\int_{x}^{x+\upsilon\tau_i} H'(x)\mathrm{d}x, \text{ by } x_0\le x\le x_0+d+\upsilon\tau_i. \quad (19)$$

The equation for the AODL output voltage obtained on the basis of (19) has the following form:

$$u_{out}(x)=c\int_{x}^{x+\upsilon\tau_i} H'(x)\mathrm{d}x, \text{ by } x_0\le x\le x_0+d+\upsilon\tau_i. \quad (20)$$

Moving to the time plane, equation (20) can be rewritten in the form:

$$u_{out}(t)=c\upsilon\int_{t}^{t+\tau_i} H'(t)\mathrm{d}t, \text{ by } \tau\le t\le\tau+\tau_0+\tau_i. \quad (21)$$

When calculating the integral in equation (21), it is necessary to distinguish three areas. The first region is characterized by the entry of an elastic wave packet into the aperture of the optical beam. In this area, the output voltage of the AODL is calculated by the formula:

$$u_{out.1}(t)=c\upsilon\int_{\tau}^{t} H'(t)\mathrm{d}t, \text{ by } \tau\le t\le\tau+\tau_i. \quad (22)$$

The second region is characterized by the process of advancing an elastic wave packet in the aperture of an optical beam. Here the calculation is performed by the equation:

$$u_{out.2}(t)=c\upsilon\int_{t-\tau_i}^{t} H'(t)\mathrm{d}t, \text{ by } \tau+\tau_i\le t\le\tau+\tau_0. \quad (23)$$

The third region is characterized by the process of the elastic wave packet exit from the aperture of the optical beam. In this area, the output voltage of the AODL is calculated by the expression:

$$u_{out.3}(t)=c\upsilon\cdot\left[\int_{\tau}^{\tau+\tau_0} H'(t)dt-\int_{\tau}^{t-\tau_i} H'(t)\mathrm{d}t\right],$$

$$\text{by } \tau+\tau_0\le t\le\tau+\tau_0+\tau_i. \quad (24)$$

The output voltage of AODL is determined on the basis of expressions (22)–(24) as the sum of three terms:

$$u_{out}(t)=u_{out.1}(t)+u_{out.2}(t)+u_{out.3}(t), \text{ by } \tau\le t\le\tau+\tau_0+\tau_i. \quad (25)$$

The formula for calculating the output voltage of the PMT is obtained from the joint analysis of equations (22)–(25) in the following form:

$$u_{out}(t)=u_{out.1}(t)\cdot[\Phi(t-\tau)-\Phi(t-\tau-\tau_i)]+$$
$$+u_{out.2}(t)\cdot[\Phi(t-\tau-\tau_i)-\Phi(t-\tau-\tau_0)]+$$
$$+u_{out.3}(t)\cdot[\Phi(t-\tau-\tau_0)-\Phi(t-\tau-\tau_0-\tau_i)],$$
$$\text{by } \tau\le t\le\tau+\tau_i+\tau_0. \quad (26)$$

Summarizing the accepted conditions, the established patterns and the results obtained, it can be postulated that when the inequality $\tau_i<\tau_0$ is fulfilled, the shape and parameters of the AODL response to a rectangular input effect can be calculated by the formula (26).

Numerical simulation of the AODL reaction to a rectangular input impact with a duration of $\tau_i=0.2$ μs, with the following parameter values: $d=1.6$ mm; $\upsilon=3.63$ km/s; $\tau=0.1$ μs.

The normalized graph of the voltage at the output of the PMT $u_{out}(t)/u_{out.max}$, constructed according to the formula (26), is shown in Fig. 5.

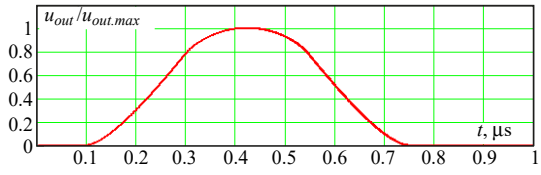

Fig. 5. The normalized graph of the voltage at the output of the AODL at the duration of the input pulse $\tau_i=0.2$ μs

From the graph in Fig. 5, it can be easily determined that the pulse duration at the output of the AODL is approximately equal to τ_0. At the same time, the shorter the duration of the input pulse, the closer the shape of the graph is to the configuration of the cross-section of the laser beam.

Now let's assume that the duration of the elastic wave packet is much less than τ_0, i. e. $\tau_i\ll\tau_0$. Under these conditions, the voltage at the output of the PMT, determined by equation (25), is formed due to the component, which is determined by equation (23). At the same time, the contributions of the components determined by equations (22) and (24) become negligibly small. For greater persuasiveness, let's repeat the above numerical simulation for the case when $\tau_i=0.01$ μs. The corresponding graph is shown in Fig. 6.

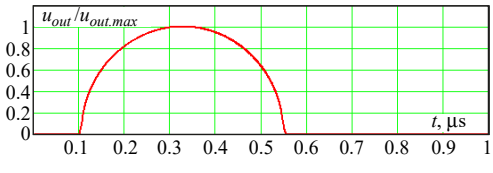

Fig. 6. Normalized graph of the voltage at the output of the AODL at the duration of the input pulse $\tau_i=0.01$ μs

From the graph in Fig. 6, it is easy to determine that the pulse duration at the output of the AODL is also equal to τ_0. However, in Fig. 5, the duration of the base of the graph is 0.64 μs, i. e. the sum $\tau_i+\tau_0$. At the same time, the duration of the bottom of the graph in Fig. 6 is equal to 0.45 μs, i. e. also the sum $\tau_i+\tau_0$. However, $\tau_i\ll\tau_0$ and therefore the shape of the graph almost repeats the configuration of the laser beam cross section. Features of the photoelastic interaction with such properties can be used to study the energy-geometric parameters of laser radiation. This issue is discussed in [21].

Thus, the results of the numerical analysis unambiguously confirm the effectiveness of formulas (18) and (26), which were obtained on the basis of the axonometric projection of the photoelastic interaction for determining the shape and calculating the parameters of the AODL response to a rectangular input action at various ratios τ_i and τ_0.

The above equations are easily modeled in the Mathcad environment, which is an obvious prerequisite for the successful application of the proposed axonometric model in the design, development and commissioning of AODL, both with direct detection and heterodyne type.

The above regularities and results of numerical simulation have been tested experimentally. The scheme of the layout for experimental studies, as well as the measuring

equipment used, is shown in Fig. 7. Here, a semiconductor laser is used as a source of coherent light. The light beam is incident into the AOM aperture at the Bragg angle. AOM is made on glassy photoelastic material TF-7 with the following parameters: $\upsilon = 3630$ m/s, $M = 5.12 \cdot 10^{-18}$ s^3/kg. As an EAT, a $LiNbO_3$ crystal with dimensions $L = 7$ mm, $H = 4$ mm and a thickness of 3 mm is used. The center frequency of the AOM is 80 MHz. In the experiments, a photodetector device based on FEU-114 developed in the laboratory was used [22].

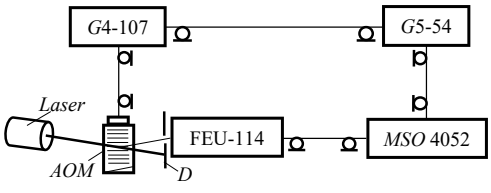

Fig. 7. Layout diagram for experimental studies

Note that, if it is necessary to implement large delays, the best results can be obtained using TeO_2 paratellurite crystals as PEM. Since, the speed of transverse waves in these materials is approximately 616 m/s. However, it should be taken into account that these materials exhibit anisotropy [23].

The rectangular pulse generated in the generator G5-54 modulates the oscillations of the high-frequency generator G4-107 (operates in external pulse modulation mode) and synchronizes the oscilloscope MSO4052. The oscillation frequency of the generator G4-107 is selected equal to the central frequency of the AOM, i. e. $f_0 = 80$ MHz. The deflected light through a slit in the diaphragm (D) falls on the photosensitive surface of the FEU-114.

The following results of theoretical studies have been experimentally tested:

1. If the duration of the rectangular pulse at the input $\tau_i > \tau_0$, then the pulse duration at the output AODL τ_{out} is equal to τ_i, and the rise time τ_r is equal to τ_0.

2. If the duration of the rectangular pulse at the input $\tau_i < \tau_0$, then the pulse duration at the output AODL τ_{out} does not depend on the duration of the input pulse and is equal to τ_0.

The voltage waveforms at the input and output of the AODL for the case $\tau_i > \tau_0$ are shown in Fig. 8. The duration of the input pulse (determined by the oscillogram at a level of 0.5 of the maximum value) is equal to $\tau_i \approx 1.0$ μs. Rise time, i. e. the time during which the output voltage changes from 0.1 to 0.9 of its maximum value is approximately 0.44 μs, which is equal to the time of crossing an optical beam with a diameter of $d = 1.6$ mm by an acoustic wave packet. The duration of the output pulse is 1.0 μs. Thus, the provisions of the first paragraph are unambiguously confirmed.

The situation for the case $\tau_i < \tau_0$ is illustrated in Fig. 9, which shows the oscillograms of the voltages at the input and output of the AODL with the above parameters.

The duration of the input pulse (determined by the oscillogram at a level of 0.5 of the maximum value) is equal to $\tau_i \approx 300$ ns. Rise time, i. e. the time during which the output voltage changes from 0.1 to 0.9 of its maximum value is approximately 300 ns, which is equal to the duration of the input pulse and fully corresponds to the above statement. The duration of the output pulse is 440 ns, which also corresponds to the above position.

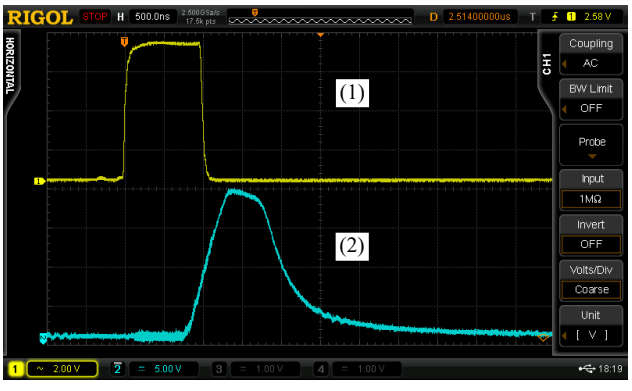

Fig. 8. Oscillograms of pulses at the input (1) and output (2) of the AODL with parameters $\tau_i \approx 1.0$ μs; $\upsilon = 3630$ m/s; $d = 1.6$ mm

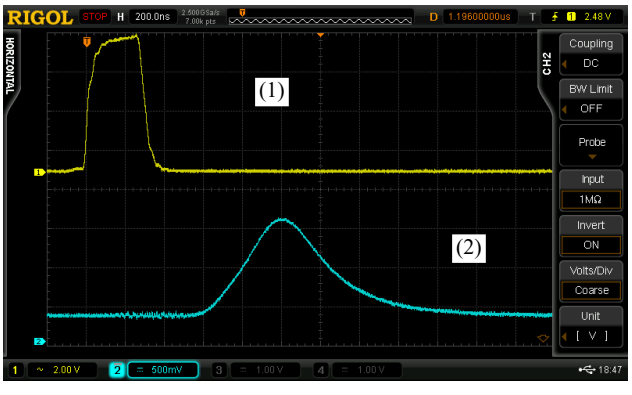

Fig. 9. Oscillograms of pulses at the input (1) and at the output (2) AODL with parameters $\upsilon = 3630$ m/s, $d = 1.6$ mm

Let's note that the duration of the output pulse shown in Fig. 9 is equal to the rise time of the output pulse shown in Fig. 8. This is due to the fact that both parameters are formed by the d/υ ratio.

Some differences between the oscillograms of the output pulse and the calculated graphs are explained by the fact that the radiation of the laser used has a round cross section and an uneven distribution of the power flux density in it. In addition to all of the above, the shape of the input pulse is not ideal.

The dependence of the duration of the output pulse τ_{out} on the duration of the input pulse τ_i was established. The graph of this dependence is shown in Fig. 10.

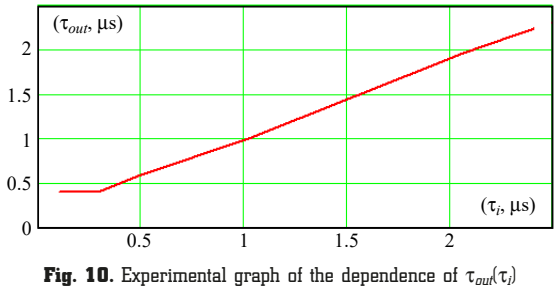

Fig. 10. Experimental graph of the dependence of $\tau_{out}(\tau_i)$

From the experimental graph in Fig. 10, the following features of the output pulse formation are obvious:

1. If the duration of the input pulse is less than the time of crossing the optical beam by an acoustic wave packet (in this case it is approximately 0.4 μs), then the duration of the output pulse is determined by the value d/υ and practically does not depend on the duration of the input pulse.

ISSN 2664-9969

2. If the duration of the input pulse is longer than the time of crossing the optical beam by an acoustic wave packet, then the duration of the output pulse is equal to the duration of the input pulse.

It should be noted that minor deviations of the experimental curve from the calculated values are mainly due to inaccuracy of measurements.

Thus, the results of experimental studies confirm the above statements and coincide with the results of numerical analysis.

3. Results and Discussion

1. According to the AODL response oscillogram (Fig. 8), the rise time τ_r of the output pulse is determined as the time during which the pulse amplitude changes from 0.1 to 0.9 from the maximum value. Then, according to the formula $f_s=\ln(0.9/0.1)/(2\pi\tau_r)=0.35/\tau_r$, the cutoff frequency of the amplitude-frequency characteristic of a specific implementation of AODL is calculated. In this case, determined by Fig. 8 rise time is $\tau_r\approx 440$ ns. Accordingly, the cutoff frequency $f_s=795$ kHz. The recommendation is valid only for the case $\tau_i>\tau_0$.

2. According to the oscillogram of the AODL response (Fig. 9), the duration of the output pulse τ_{out} is determined, at the level of 0.5 of the maximum value. Then the real diameter of the light beam is calculated using the formula $d=\upsilon\cdot\tau_{out}$. In this case, the duration of the output pulse, determined by Fig. 9, is $\tau_{out}\approx 440$ ns. Accordingly, the actual diameter of the light beam is $d\approx 1.6$ mm. The recommendation is valid only for the case of $\tau_i<\tau_0$.

There are no restrictions on the use of the developed axonometric model. It is applicable both for direct detection AODL's and for the heterodyne type. In all cases, only the limiting conditions listed above must be met.

4. Conclusions

The axonometric model of photoelastic interaction improves the spatial representation of this physical process and greatly simplifies the calculation of the response parameters of AODL with specified design characteristics and parameters to the input effect in the form of a rectangular pulse. In this case, three parameters are decisive: the duration of the input pulse, the velocity of propagation of the elastic wave in the PEM and the diameter of the light beam. The ratio of these parameters uniquely determines the shape and parameters of the AODL output signal. By simple calculations, it can be easily established that the proposed model is equally valid for all types of AODL with direct detection and heterodyne type.

Based on the results of numerical modeling and experimental approbation, two postulates are formulated:

1) if the pulse duration at the AODL input is longer than the time of intersection of the optical beam by an elastic wave packet, then the duration of the output pulse is equal to the duration of the input pulse;

2) if the duration of the pulse at the input of the AODL is less than the time of crossing the optical beam by the elastic wave packet, then the duration of the output pulse is equal to the time of crossing the optical beam by the elastic wave packet.

According to the oscillogram of the output response of a specific implementation of the AODL, it is possible to determine both the cutoff frequency and the diameter of the light beam incident on the surface of the photodetector. To do this, it is enough to choose $\tau_i>\tau_0$ and $\tau_i<\tau_0$, respectively.

Conflict of interest

The author declares that they have no conflict of interest in relation to this research, whether financial, personal, authorship or otherwise, that could affect the research and its results presented in this paper.

Financing

Presentation of research in the form of publication through financial support in the form of a grant from SUES (Support to Ukrainian Editorial Staff).

Data availability

The manuscript has no associated data.

References

1. Mandal, J., Mandal, M. K. (2019). An Electronically Tunable Delay Line With Continuous Control of Slope and Peak Delay. *IEEE Transactions on Microwave Theory and Techniques, 67 (12),* 4682–4691. doi: https://doi.org/10.1109/tmtt.2019.2947474
2. Manzaneque, T., Lu, R., Yang, Y., Gong, S. (2019). Low-Loss and Wideband Acoustic Delay Lines. *IEEE Transactions on Microwave Theory and Techniques, 67 (4),* 1379–1391. doi: https://doi.org/10.1109/tmtt.2019.2900246
3. Kao, S.-K. (2020). Multi-phases all-digital DLL with multi-input and wide-range delay line. *International Journal of Electronics, 108 (3),* 345–360. doi: https://doi.org/10.1080/00207217.2020.1793416
4. Kim, K., Moon, H., Chung, Y. (2016). Tunable Optical Delay Line Based on Polymer Single-Ring Add/Drop Filters and Delay Waveguides. *Korean Journal of Optics and Photonics, 27 (5),* 174–180. doi: https://doi.org/10.3807/kjop.2016.27.5.174
5. Pavan, S., Klumperink, E. (2018). Analysis of the Effect of Source Capacitance and Inductance on N-Path Mixers and Filters. *IEEE Transactions on Circuits and Systems I: Regular Papers, 65 (5),* 1469–1480. doi: https://doi.org/10.1109/tcsi.2017.2754342
6. Diewald, A. R., Steins, M., Müller, S. (2018). Radar target simulator with complex-valued delay line modeling based on standard radar components. *Advances in Radio Science, 16,* 203–213. doi: https://doi.org/10.5194/ars-16-203-2018
7. Li, M.-H., Lu, R., Manzaneque, T., Gong, S. (2020). Low Phase Noise RF Oscillators Based on Thin-Film Lithium Niobate Acoustic Delay Lines. *Journal of Microelectromechanical Systems, 29 (2),* 129–131. doi: https://doi.org/10.1109/jmems.2019.2961976
8. Chen, W., Zhu, D., Pan, S. (2018). Compact photonic triangular waveform generator with wideband tunability. *Optical Engineering, 57 (10),* 1. doi: https://doi.org/10.1117/1.oe.57.10.106106
9. Shakin, O. V., Nefedov, V. G., Churkin, P. A. (2018). Aplication of Acoustooptics in Electronic Devices. *Wave Electronics and its Application in Information and Telecommunication Systems.* Saint Petersburg, 340. doi: https://doi.org/10.1109/weconf.2018.8604351
10. Yushkov, K. B., Molchanov, V. Ya., Ovchinnikov, A. V., Chefonov, O. V. (2017). Acousto-optic replication of ultrashort laser pulses. *Physical Review A, 96 (4).* doi: https://doi.org/10.1103/physreva.96.043866
11. Schubert, O., Eisele, M., Crozatier, V., Forget, N., Kaplan, D., Huber, R. (2013). Rapid-scan acousto-optical delay line with 34 kHz scan rate and 15 as precision. *Optics Letters, 38 (15),* 2907–2910. https://doi.org/10.1364/ol.38.002907
12. Chandezon, J., Rampnoux, J.-M., Dilhaire, S., Audoin, B., Guillet, Y. (2015). In-line femtosecond common-path interferometer in reflection mode. *Optics Express, 23 (21),* 27011–27019. doi: https://doi.org/10.1364/oe.23.027011

13. Gasanov, A. R., Gasanov, R. A., Akhmedov, R. A., Sadykhov, M. V. (2021). Optimization of the Operational Parameters of an Acousto-Optical Delay Line. *Instruments and Experimental Techniques, 64 (3),* 415–419. doi: https://doi.org/10.1134/s0020441221020135
14. Hasanov, A. R., Hasanov, R. A. (2017). Some peculiarities of the construction of an acousto-optic delay line with direct detection. *Instruments and Experimental Techniques, 60 (5),* 722–724. doi: https://doi.org/10.1134/s0020441217050062
15. Balakshiy, V. I., Parygin, V. N., Chirkov, L. E. (1985). *Physical foundations of acousto-optics*. Moscow: Radio and communication, 278.
16. Davis, C. C. (2014). *Lasers and Electro-optics*. Cambridge University Press, 720. doi: https://doi.org/10.1017/cbo9781139016629
17. Gasanov, A. R., Gasanov, R. A., Akhmedov, R. A. (2021). Analysis of Amplitude-Frequency Response of Acousto-Optic Delay Line. *Radioelectronics and Communications Systems, 64 (1),* 36–44. doi: https://doi.org/10.3103/s0735272721010040
18. Lee, J. N., Vanderugt, A. (1989). Acoustooptic signal processing and computing. *Proceedings of the IEEE, 77 (10),* 1528–1557. doi: https://doi.org/10.1109/5.40667
19. Hasanov, A. R., Hasanov, R. A., Ahmadov, R. A., Agayev, E. A. (2019). Time- and Frequency-Domain Characteristics of Direct-Detection Acousto-Optic Delay Lines. *Measurement Techniques, 62 (9),* 817–824. doi: https://doi.org/10.1007/s11018-019-01700-3
20. Hasanov, A. R., Hasanov, R. A., Akhmedov, R. A., Sadikhov, M. V. (2021). Functionality of the Acousto-Optic Delay Lines outside the Cutoff Frequency. *Russian Microelectronics, 50 (7),* 566–570. doi: https://doi.org/10.1134/s1063739721070143
21. Gasanov, A. R., Gasanov, R. A., Akhmedov, R. A., Agaev, E. A. (2020). An Acousto-Optic Method for Measuring the Energy-Geometric Parameters of Laser Radiation. *Instruments and Experimental Techniques, 63 (2*), 234–237. doi: https://doi.org/10.1134/s0020441220020098
22. Hasanov, R. A. (2015). Photodetectors for acousto-optic delay lines. Instruments and Systems. *Monitoring, Control, and Diagnostics, 12,* 31–36.
23. Akhmedzhanov, F., Mirzaev, S., Saidvaliev, U. (2018). Singularities of anisotropy of acoustic attenuation in paratellurite crystals. *Proceedings of Meetings on Acoustics*. doi: https://doi.org/10.1121/2.0000937

✉ ***Afig Hasanov,*** *Doctor of Technical Science, Professor, Azerbaijan National Aviation Academy, Baku, Azerbaijan, ORCID: https://orcid.org/0000-0003-4141-5969, e-mail: afig.gasanov.51@mail.ru*

Ruslan Hasanov, *Doctor of Technical Science, Associate Professor, Azerbaijan National Aviation Academy, Baku, Azerbaijan, ORCID: https://orcid.org/0000-0003-3419-8599*

Asad Rustamov, *PhD, Professor, Azerbaijan National Aviation Academy, Baku, Azerbaijan, ORCID: https://orcid.org/0000-0002-4456-6626*

Elgun Agayev, *PhD, Senior Lecturer, Azerbaijan National Aviation Academy, Baku, Azerbaijan, ORCID: https://orcid.org/0000-0002-9861-2624*

Vugar Eynullayev, *PhD, Senior Lecturer, Azerbaijan National Aviation Academy, Baku, Azerbaijan, ORCID: https://orcid.org/0000-0002-1097-6053*

Rovshan Ahmadov, *PhD, Lecturer, Azerbaijan National Aviation Academy, Baku, Azerbaijan, ORCID: https://orcid.org/0000-0002-5731-695X*

Masud Sadikhov, *Doctoral Student, Azerbaijan National Aviation Academy, Baku, Azerbaijan, ORCID: https://orcid.org/0000-0002-0039-9942*

✉ *Corresponding author*